sustainability

MDPI

Article

Lane Allocation Optimization in Container Seaport Gate System Considering Carbon Emissions

Zhihong Jin [1], Xin Lin [2,†], Linlin Zang [1], Weiwei Liu [3,*] and Xisheng Xiao [4]

1 Transportation Engineering College, Dalian Maritime University, Dalian 116026, China; jinzhihong@dlmu.edu.cn (Z.J.); lorrine6@163.com (L.Z.)
2 School of Management, Zhejiang University, Hangzhou 310058, China; linx612@zju.edu.cn
3 School of Economics and Management, Dalian University of Technology, Dalian 116024, China
4 Bigdata Technology Institute, Guizhou Light Industry Polytechnic College, Guiyang 550025, China; shiauxsh@126.com
* Correspondence: liuweiwei887145@mail.dlut.edu.cn
† Xin Lin is the co-first author and Zhejiang University is the co-first research institute of the paper.

Abstract: Long queues of arrival trucks are a common problem in seaports, and thus, carbon emissions generated from trucks in the queue cause environmental pollution. In order to relieve gate congestion and reduce carbon emissions, this paper proposes a lane allocation framework combining the truck appointment system (TAS) for four types of trucks. Based on the distribution of arrival times obtained from the TAS, lane allocation decisions in each appointment period are determined in order to minimize the total cost, including the operation cost and carbon emissions cost. The resultant optimization model is a non-linear fractional integer program. This model was firstly transformed to an equivalent integer program with bilinear constraints. Then, an improved branch-and-bound algorithm was designed, which includes further transforming the program into a linear program using the McCormick approximation method and iteratively generating a tighter outer approximation along the branch-and-bound procedure. Numerical studies confirmed the validity of the proposed model and algorithm, while demonstrating that the lane allocation decisions could significantly reduce carbon emissions and operation costs.

Keywords: container seaport; carbon emissions; lane allocation; truck appointment system; infrastructure scheduling; fractional integer programming; branch-and-bound algorithm

Citation: Jin, Z.; Lin, X.; Zang, L.; Liu, W.; Xiao, X. Lane Allocation Optimization in Container Seaport Gate System Considering Carbon Emissions. *Sustainability* **2021**, *13*, 3628. https://doi.org/10.3390/su13073628

Academic Editor: Maxim A. Dulebenets

Received: 31 January 2021
Accepted: 16 March 2021
Published: 24 March 2021

1. Introduction

With the development of economic globalization and the fast growth of international trade, maritime transportation plays an increasingly important role in the international supply chain [1,2]. As a result of the continuous increase in container shipments, the working intensity of seaports has been increasing, and long queues in the gate system have become a serious problem in seaport operations management. Arrival trucks must wait for a long time before entering the gate. The more time the trucks spend in the gate, the greater the operational challenge for container seaports. For container seaports, there is the risk that ships will not sail on schedule if the trucks do not deliver or collect containers punctually. In terms of the truck companies, waiting too long leads to a low turnover efficiency and limits the daily task capacity of trucks. For society, a large amount of greenhouse gas emissions are generated as a consequence of the extra fuel consumed by trucks that are idling or moving at a low speed in the queue, leading to environmental pollution at the seaport.

Combatting global warming is an integral goal for society as a whole. Nowadays, governments have introduced energy-efficient measures to control carbon emissions. The carbon tax mechanism is considered as one of the most important methods of developing a low-carbon economy. Finland was the first country to impose the carbon emission tax in the world. The UK initiated the "floor carbon price" mechanism in 2013, that involved setting a lower limit on the price of carbon. At the end of 2018, the New Zealand government decided to strengthen the operation of the carbon trading system in order to achieve the contribution goal set by the nationally determined allowances. The International Maritime Organization (IMO) has also responded actively to reduce carbon emissions. The IMO claims that the greenhouse gas emissions produced by international shipping will increase by 50–250% in the next 30 years, without efforts to limit emissions [3]. In order to shoulder social responsibility, the IMO promises to take certain measures, e.g., imposing a carbon tax and promoting the innovation of green shipping equipment, in order to cut emissions by 50% by 2050 [4]. National maritime authorities have established appropriate regulations to limit high-emission activities in seaports. Reducing carbon emissions has drawn the attention of scholars. There are a number of published studies on low carbon and sustainability in fleet deployment [5–8], berth allocation [9–12], quay crane planning [12–15], yard management [16,17] and dry port deployment [18–20]. How to shorten the queue time and guide trucks to move faster in order to relieve congestion in the gate has become a necessary breakthrough to achieve the green management of seaports.

Two components of seaports directly affect congestion in the gate system, namely, the truck appointment system (TAS) and lane allocation planning. The TAS is a widely used system for appointing the period at which trucks can enter the gate, where the opening time of gate, appointment periods and service quota within each appointment period are provided. Some international ports, such as Rotterdam, Shanghai, and Dalian, require trucks to make an appointment 24 h in advance [21]. Trucks can choose the expected arrival period. If there are no available slots in in the expected period, the seaport will require the trucks to choose another period. Thus, the TAS can guide the arrival trucks from the peak period to the off-peak period to some extent [22]. However, it also causes tedious smartphone app operations and represents an irritating experience for truck drivers in the event that they unfortunately appoint the arrival time in an overflow appointment period. Therefore, there is a need for the efficient allocation of lane resources in order to balance arrival flows of different types of trucks. The paper designs a framework to combine the lane allocation problem with TAS (see Figure 1) to try to figure out an effective green lane allocation policy for seaport operations.

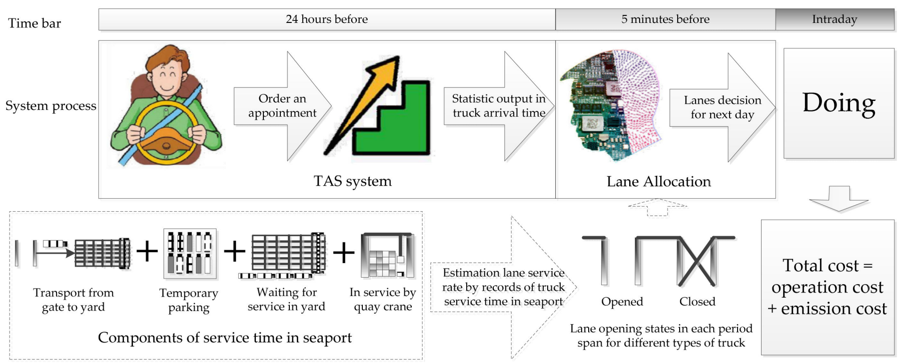

Figure 1. A lane allocation framework combining truck appointment system (TAS).

As shown in Figure 1, based on the data recorded in TAS, the distribution of the arrival time can be obtained. This is a typical process that transforms the data into useful information. The time each truck spent in the seaport consists of four parts: the transport time from gate to yard, the temporary parking time, the waiting time in the yard and the in-service time by the quay crane. The service time for the trucks is recorded by RFID (Radio Frequency Identification) [23,24] and stored in the seaport information management system, which could be used to estimate the service rate of lanes. With the distribution of arrival time and the service rate of lanes, the opening planning of lanes for different types of trucks in each appointment period is made, in order to minimize the total cost including the carbon emissions cost and operation cost. The green lane allocation model is established, which is a nonlinear fractional integer programming. Firstly, it can be equivalently transformed into an integer programming with bilinear constraints. Furthermore, an improved branch-and-bound algorithm is designed, which includes transforming the relaxation programming into a linear program by the McCormick approximation method and iteratively generating tighter outer approximation in the branch-and-bound tree. A numerical study shows the effectiveness of the proposed model and algorithm, and demonstrates that the resulting lane allocation policy could relieve congestion and reduce carbon emissions.

The rest of this paper is organized as follows: Section 2 reviews the related literature. Section 3 describes the lane allocation problem and proposes the lane allocation model. Section 4 equivalently transforms the model and proposes an improved branch-and-bound algorithm. The numerical results of a case study of a seaport in the south of China are reported in Section 5. Conclusions and future research directions are outlined in Section 6.

2. Literature Review

Resource allocation in the seaport mainly involves three subsystems, namely berth, yard and gate. In the berth subsystem, the resources are berth and shore crane. The studies about berth allocation usually consider them together [10,25]. In the yard subsystem, the slot stores a specific container and the quay crane are used to load, discharge and overturn. Li et al. [26] studied the quay crane allocation problem and proposed a non-dominated genetic algorithm II-based approach to solve it. Fan et al. [27] considered the external yard slot allocation in a multi-ports truck scheduling problem. In the gate subsystem, Yu and Zhou [28] studied the lane allocation problem in the daily plan ignoring the types of trucks. Facchini et al. [18] proposed to allocate several dry ports inland to take on a part of container handling tasks of the seaport yard system, in order to improve operations efficiency and reduce congestion for the seaport.

Nowadays, with the enhancement of environmental consciousness, much importance is attached to carbon emissions in seaports by IMO and governments. Recent studies haven taken green resource allocation into account [5–8]. For research on green berth allocation, Du et al. [9] concerned the vessel emissions generated by fuel consumption in the berth allocation problem. Zhen et al. [10] considered the uncertain arrival time of vessels and workloads of shore crane in the berth allocation problem with the objective of minimizing the carbon taxation cost. Venturini et al. [11] studied the speed-based vessel berth matching problem in multi-ports. Sun et al. [12] proposed a berth allocation problem considering quay crane pre-scheduling with the objective of minimizing the carbon taxation cost. For research on green yard management, Talavera et al. [13] found that the quay crane emission played an important role in the seaport emissions. Based on the actual quay crane data in Shanghai Yangshan Deep Water Port (SYDWP), Sha et al. [14] studied the crane moving problem with the objective of minimizing fuel consumption. Peng et al. [15] formulated a green quay crane scheduling problem in a yard network. Except for the quay crane, the carbon emissions from the transport equipment in yard the subsystem—such as inner trucks and automated guided vehicles (AGVs)–were considered in Kavakeb et al. [16] and Yu et al. [17]. For green lane allocation in the gate subsystem, Yu et al. [28] studied the lane allocation problem, but they did not consider carbon emissions. Facchini et al. [18], Digiesi et al. [19] and Kurtulus and Cetin [20] considered carbon emissions due to containers handing, but they focused on dry ports. Lane allocation in seaports influences the queue length of trucks and is thus closely related to large amounts of carbon emissions generated due to the low speed moving or engine idling of trucks. This paper focuses on lane allocation problem with the consideration of carbon emissions. Most studies above used fuel consumption factors or carbon emissions factors to measure carbon emissions. In contrast, we propose a simplified and tractable measure method based on the carbon emissions cost involving the speed, weight and engine of trucks in Bektas and Laporte [29] and Ricke et al. [30].

As the bridge between trucks and seaports, the TAS has drawn a great deal of attention in recent years. There is extended research on the one-way appointment mechanism and multi-time appointment mechanism. For research on the one-way appointment mechanism, Zeng et al. [31] studied the optimal quota in each appointment period by using the fluid flow-based pointwise stationary approximation (PSFFA) on the basis of the genetic algorithm. Ma et al. [32] considered the storage capacity and queue length upper bound constraints in a quota optimization problem with a dependent time window. They designed a hybrid genetic algorithm based on simulated annealing method. Phan and Kim [33] explored the congestion rates and verified that a pricing toll mechanism, such as an additional entrance fee in peak periods or in late arrival periods, could effectively relieve congestion in seaports. Im et al. [34] considered the truck waiting time and the container rehandling time in a TAS optimization model. For research on a multi-time appointment mechanism, Li et al. [35] introduced the concept of disruption management to construct a robust interruption recovery appointment mechanism. Shao et al. [36] and Yang et al. [22] proposed a second time appointment mechanism, that is order–reject–reorder–accept. However, the multi-time appointment could cause interference to the daily scheduling of truck companies [37]. Thus, this paper also adopts the commonly used one-way appointment mechanism.

At present, most studies on green resources allocation in seaports concentrate on the berth subsystem and yard subsystem. In comparison, lane allocation in the gate subsystem draws less attention. However, the congestion problem and the resultant carbon emissions problem have become serious problems in seaport management. In view of this problem, we studied the green lane allocation problem combing with TAS. The green lane allocation optimization model was established with the objective of minimizing the total cost, including the operation cost and carbon emissions cost. We designed an improved branch and bound to solve the model in order to obtain the optimal lane allocation decisions.

3. The Green Lane Allocation Model

3.1. Problem Description

This paper considered green lane allocation with the consideration of carbon emissions generated by trucks in the gate. There are four types of trucks: sending loaded container (SL), sending empty container (SE), taking loaded container (TL) and taking empty container (TE). Under the TAS, the seaport divided the day into equal appointment periods. For example, if there are six appointment periods during a day, then the span of each appointment period is 4 h. Each truck is required to appoint one period to arrive at the seaport 24 h in advance. When each truck arrives at the gate in the appointment period, this truck could choose any available lane to join the queue, if any, to wait for service.

Figure 2 shows the operation flow of a gate system. There are four lanes available at the gate. In the appointment period (04:00, 08:00), the gate system opens only one lane to serve trucks of type TE (Suppose Lane A) and three lanes to serve trucks of type SL (Suppose Lane B, Lane C, Lane D). Each truck of type TE joins the queue of Lane A to enter the seaport. Each truck of type SL could choose the shortest queue between Lane B, Lane C, and Lane D to enter the seaport. The waiting time in lane could be different for each truck. The trucks are idling during queuing at the gate, thus generating carbon emissions. The opening of lanes leads to the operation cost of seaport.

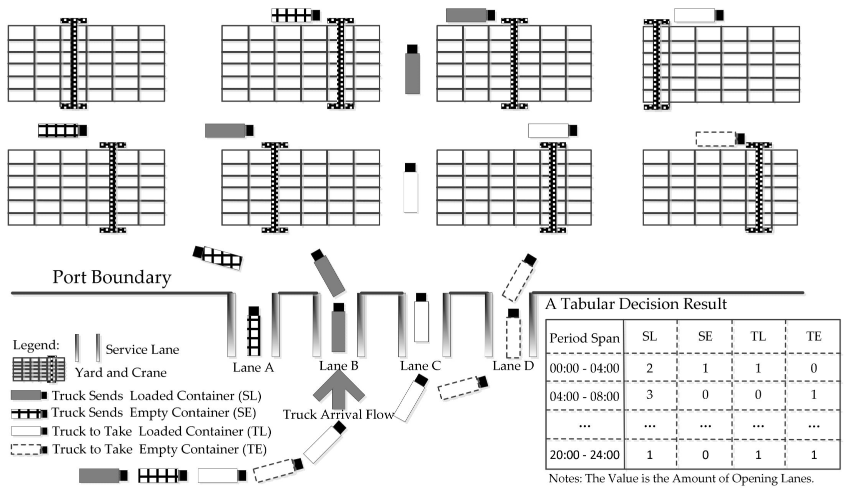

Figure 2. Operation flow of gate system.

3.2. Assumptions

The green lane allocation model is based on the following assumptions:

- Truck arrival process: Under the TAS collection, each truck appoints the expected arrival period, not the exact arrival time. Due to the individual driving habit of different truck drivers and unknown urban traffic congestion, the arrival process of each type of truck in each appointment period is the Poisson process and the interval time between any two trucks of the same type obeys independent and identically exponential distribution.
- Lane service process: The service for trucks in each lane follows a first-come-first-served basis. The lane could not serve the next truck until the truck before has been served. Due to the interval time between any two trucks of the same type obeying exponential distribution, the service time for each type of trucks obeys independent and identically exponential distribution.
- Lane operational rule: The switching time for serving different types of trucks between adjacent appointment periods is sufficiently short. The switching costs could be negligible in seaport operation.

3.3. Parameters and Variables

The green lane allocation model defines the following symbols:

- Parameters: I: The set of types of trucks, $i = 1, 2, 3, 4$ respectively, denote trucks for SL, SE, TL and TE; T: The set of appointment periods; c_i: The average operation cost of lanes in service for trucks of type i, USD/hour; c_o: The average carbon emissions cost, USD/hour; g: The scale of lanes in the gate system; λ_{it}: The average number of trucks of type i in unit time of appointment period t, truck/hour; μ_i: The average service rate of lanes for trucks of type i, truck/hour; t_0: The span of each appointment period, hour.
- Decision Variables: N_{it}: The number of lanes available for trucks of type i in appointment period t.

3.4. Mathematical Model

3.4.1. Structure of Objective Function

(1) The operation cost

The lanes that incur the operation cost mainly refer to serving all types of trucks. The operation cost can be expressed as

$$C_1 = \sum_{t=0}^{|T|} \sum_{i=1}^{4} c_i t_0 N_{it} \tag{1}$$

(2) The carbon emissions cost

The carbon emissions cost is related to the average queue length of trucks, the average carbon emissions cost of each truck and the average number of arrival trucks in each appointment period. Therefore, the queueing structure of trucks is an $M/M(N_{jt})/1$ system, the average queue length can be obtained, which is $\frac{\lambda_{it}}{N_{it}\mu_i(N_{it}\mu_i-\lambda_{it})}$. Thus, the carbon emissions cost can be expressed as

$$C_2 = \sum_{t=0}^{|T|} \sum_{i=1}^{4} c_o \lambda_{it} t_0 \frac{\lambda_{it}}{N_{it}\mu_i(N_{it}\mu_i - \lambda_{it})} \tag{2}$$

3.4.2. Optimize Model Settings

Based on the cost considered in Section 3.4.1, the green lane allocation model is formulated as follows:

Model (a)

$$\min \sum_{t=0}^{|T|} \sum_{i=1}^{4} c_i t_0 N_{it} + \sum_{t=0}^{|T|} \sum_{i=1}^{4} c_o \lambda_{it} t_0 \frac{\lambda_{it}}{N_{it}\mu_i(N_{it}\mu_i-\lambda_{it})} \tag{3}$$

s.t.

$$\sum_{i=1}^{4} N_{it} \le g,\ \forall t \in T \tag{4}$$

$$\frac{\lambda_{it}}{N_{it}\mu_i} < 1,\ \forall t \in T,\ i \in I \tag{5}$$

$$N_{it} \in Z^+,\ \forall t \in T,\ i \in I \tag{6}$$

The objective function (3) minimizes the total cost, which is the sum of the operation cost and carbon emissions cost. Constraints (4) ensure that the number of lanes available for all types of trucks in appointment period t should be less than the scale of lanes. Constraints (5) ensure that the average number of trucks of type i arriving at the lanes in appointment period t does not exceed the average service capacity. Constraints (6) enforce that the decision variables are integer.

Model (a) is a fractional integer programming, which is difficult to solve directly. Then, we further analyze model (a) and propose an efficient algorithm to solve it.

4. An Improved Branch-and-Bound Algorithm

Fractional programming is a class of non-convex nonlinear mathematical programming problem. There may be multiple non-global optimal solutions for fractional programming. There is no existing general global convergence criterion, which makes it difficult to solve the fractional programming problem. In addition, if the decision variables are integer, then solving the fractional integer program is more challenging. We first transformed the fractional integer programming into a discrete programming with linear objective and bilinear constraints (Section 4.1). We then proposed an improved branch-and-bound algorithm, including further the transformation of the program relaxation into a mixed-integer linear program by the McCormick approximation method and iteratively generating tighter outer approximation in the branch-and-bound tree.

4.1. Equivalent Transformation of Fractional Integer Programming

For the fractional objective function in model (a), by introducing the variable $W_{it} = \frac{1}{N_{it}\mu_i(N_{it}\mu_i-\lambda_{it})} (\forall t \in T,\ i \in I)$, model (a) can be equivalently transformed into the following model:

Model (b)

$$\min \sum_{t=0}^{|T|} \sum_{i=1}^{4} c_i t_0 N_{it} + \sum_{t=0}^{|T|} \sum_{i=1}^{4} c_o \lambda_{it}^2 t_0 W_{it} \tag{7}$$

s.t. Equation (4)–(6)

$$W_{it} = \frac{1}{N_{it}\mu_i(N_{it}\mu_i - \lambda_{it})}, \forall t \in T,\ i \in I \tag{8}$$

$$W_{it} > 0,\ \forall t \in T,\ i \in I \tag{9}$$

The objective function of model (b) is linear, but there are still fractional constraints (8). By introducing variable $\alpha_{it} = W_{it}N_{it}$ and $\beta_{it} = N_{it}\alpha_{it}$ $(\forall t \in T,\ i \in I)$, constraints (8) can be transformed into ${\mu_i}^2\beta_{it} - \mu_i\lambda_{it}\alpha_{it} = 1$. Thus, the following equivalent model can be obtained:

Model (c)
min Equation (7)
s.t. Equation (4)–(6), (9)

$${\mu_i}^2\beta_{it} - \mu_i\lambda_{it}\alpha_{it} = 1,\ \forall t \in T,\ i \in I \tag{10}$$

$$\alpha_{it} = W_{it}N_{it}, \forall t \in T, i \in I \tag{11}$$

$$\beta_{it} = N_{it}\alpha_{it}\ , \forall \in T, i \in I \tag{12}$$

$$\alpha_{it},\ \beta_{it} > 0,\ \forall \in T, i \in I \tag{13}$$

Compared with model (a), there are no fractional terms in model (c), thus reducing the complexity of solving the problem to some extent. However, there are still bilinear functions in constraints (11) and (12), which makes solving model (c) a challenge.

4.2. Algorithm Designing

In this section, we design an improved branch-and-bound algorithm to solve (c). In the framework of branch-and-bound algorithm, we started solving the continuous relaxation programming of model (c), that is:

Model (d)
min Equation (7)
s.t. Equation (4)–(6), (9)–(13)

$$N_{it} \in R^+\ , \forall t \in T,\ i \in I \tag{14}$$

For the bilinear functions in constraints (11) and (12), we adopted McCormick approximation method to linearize them. McCormick envelope is the tightest convex hull of bilinear function [38].

Lemma 1. *For the points (x, y, xy) such that (x, y) belongs to the rectangle $[l_x, u_x] \times [l_y, u_y]$, their convex hull is equivalent to the set of points that satisfy the following McCormick inequalities:*

$$\begin{cases} w_{xy} \le l_x y + u_y x - l_x u_y \\ w_{xy} \le u_x y + l_y x - u_x l_y \\ w_{xy} \ge l_x y + l_y x - l_x l_y \\ w_{xy} \ge u_x y + u_y x - u_x u_y \end{cases} \tag{15}$$

By Lemma 1, the envelopes of bilinear functions in constraints (11) and (12), respectively, are:

$$\alpha_{it} \le l_{W_{it}}N_{it} + u_{N_{it}}W_{it} - l_{W_{it}}u_{N_{it}},\ \forall t \in T,\ i \in I \tag{16}$$

$$\alpha_{it} \le u_{W_{it}}N_{it} + l_{N_{it}}W_{it} - u_{W_{it}}l_{N_{it}},\ \forall t \in T,\ i \in I \tag{17}$$

$$\alpha_{it} \ge l_{W_{it}}N_{it} + l_{N_{it}}W_{it} - l_{W_{it}}l_{N_{it}}\ ,\ \forall t \in T,\ i \in I \tag{18}$$

$$\alpha_{it} \ge u_{W_{it}}N_{it} + u_{N_{it}}W_{it} - u_{W_{it}}u_{N_{it}},\ \forall t \in T,\ i \in I \tag{19}$$

and:

$$\beta_{it} \le l_{N_{it}}\alpha_{it} + u_{\alpha_{it}}N_{it} - l_{N_{it}}u_{\alpha_{it}},\ \forall t \in T,\ i \in I \tag{20}$$

$$\beta_{it} \le u_{N_{it}}\alpha_{it} + l_{\alpha_{it}}N_{it} - u_{N_{it}}l_{\alpha_{it}},\ \forall t \in T,\ i \in I \tag{21}$$

$$\beta_{it} \ge l_{N_{it}}\alpha_{it} + l_{\alpha_{it}}N_{it} - l_{N_{it}}l_{\alpha_{it}},\ \forall t \in T,\ i \in I \tag{22}$$

$$\beta_{it} \ge u_{N_{it}}\alpha_{it} + u_{\alpha_{it}}N_{it} - u_{N_{it}}u_{\alpha_{it}},\ \forall t \in T,\ i \in I \tag{23}$$

Thus, the relaxation programming (d) can be transformed into the following model
Model (e)
min Equation (7)
s.t. Equation (4)–(6), (9) and (10), (13) and (14), (16)–(23)

Compared with model (d), model (e) becomes a linear program which is easy to deal with, reducing the complexity of solving model (d).

If the relaxation program (e) is infeasible, then we conclude that the original problem is infeasible. Otherwise, we need to determine a branching variable to generate two subproblems. Let LP_k denote the subproblem, where k represents the current node, $\overline{N_{jt}}^k$ and $z_{\ LP_k}$ denote the optimal solution and the associated optimal objective function value, respectively. If $\overline{N_{j't'}}^k$ is a nonintegral value, then we can branch on $\overline{N_{j't'}}^k$ to, respectively, add $N_{j't'} \le \left\lfloor \overline{N_{j't'}}^k \right\rfloor$ and $N_{j't'} \ge \left\lfloor \overline{N_{j't'}}^k + 1 \right\rfloor$ to LP_k to create two subproblems. To create tighter outer approximations, after branching each time, we need to refine envelopes (16)–(23) in the two resulting subproblems.

After solving LP_k, we can fathom nodes in the branch-and-bound tree if one condition holds:

(1) If LP_k is infeasible, there are no feasible points. Then, this node can be fathomed.
(2) If LP_k produces an integer solution, this node can be fathomed. If $z_{\ LP_k} < U$, where U is the current upper bound, then update $U = z_{\ LP_k}$.
(3) If LP_k produces a non-integer solution, and if $z_{\ LP_k} \le\ L$, where L is the current lower bound, there is no better solution. Then, this node can be fathomed.

Summarizing the above, the improved branch-and-bound algorithm is stated below:
Step 1: Initialize $U = +\infty$, $L = -\infty$, $k = 1$, and choose a tolerance $\varepsilon > 0$
Step 2: Solve LP_k, if LP_k is infeasible, fathom this node, else obtain $\overline{N_{jt}}^k$ and $z_{\ LP_k}$
Step 2.1: If $\overline{N_{jt}}^k$ is integer, fathom this node
Step 2.1.1: If $z_{\ LP_k} < U$, update $U = z_{\ LP_k}$, then new incumbent $N^*_{jt} = \overline{N_{jt}}^k$;
Step 2.2: If $\overline{N_{jt}}^k$ is non-integer
Step 2.2.1: If $z_{\ LP_k} \le L$, fathom this node
Step 2.2.2: If $z_{\ LP_k} > L$, randomly choose a variable $\overline{N_{j't'}}^k$ with non-integral value to branch, then respectively add $N_{j't'} \le \left\lfloor \overline{N_{j't'}}^k \right\rfloor$ and $N_{j't'} \ge \left\lfloor \overline{N_{j't'}}^k + 1 \right\rfloor$ to LP_k to create two subproblems, and refine the envelopes (16)–(23) in the resultant two subproblems
Step 3: Set $k = k + 1$, then go to step 2
Step 4: Return the optimal solution N^*_{jt}.

5. Numerical Study

5.1. Numerical Settings

The numerical study selects a container seaport in the south of China. RFID [20,21] recorded the TAS data of this container seaport from 10 October 2020 to 10 November 2020, which contain 83,582 records. These records include information of trucks, e.g., arrival time, in-port time, off-port time, the average tractor weight, the average container weight in loaded, the average container weight in empty, and engine working parameters. The gate system has eight lanes available to serve trucks. The numbers of four types of trucks each 4 h form 0:00 a.m. within a day are illustrated in Table 1, including the maximum number, minimum number and average number. In addition, the numbers of each type of trucks each hour during a day are recoded, which is depicted in Figure 3.

Table 1. Number of four types of trucks each four hours during a day.

Arrival Number	SL	SE	TL	TE
Max.	204	156	168	119
Min.	68	34	71	90
Average	134	103	119	109

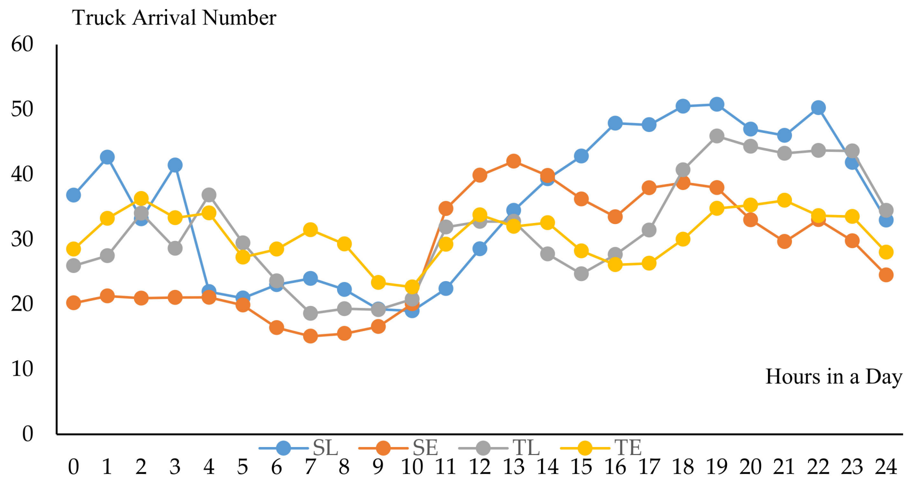

Figure 3. Truck arrival flow during a day.

5.1.1. Seaport Operational Settings

This section analyzes the service time (i.e., off-port time minus in-port time) spent by each type of trucks in port by using the Kolmogorov–Smirnov (K–S) test in the SPSS 16.0 software. As results showed in Table A1 in Appendix A, the absolute distances are all less than 0.3 and all of the asymptotic significances are not more than 0.05. That is, the exponential distribution of the service time in port for all types of trucks passes the K–S test in the confidence threshold of 95%. The service rate of all types of trucks was listed in Table 2 below.

Table 2. Service rate.

Type of Trucks	SL	SE	TL	TE
Service Rate (truck/hour)	19.11	24.90	15.92	23.62

Based on the data, the unit operation cost is listed in Table 3 below.

Table 3. Unit operation cost.

Type of Trucks	SL	SE	TL	TE
Operation Cost (USD/hour)	20.01	16.95	22.05	14.12

5.1.2. Appointment Period Settings in TAS

The span of appointment period in the data is 4 h. We use the Kolmogorov–Smirnov (K–S) test in SPSS 16.0 software to analyze the distribution of truck arrival flow in appointment period with span (1, 2, 3, 6 h). As results showed in in Table A2 in Appendix A, the exponential distribution of all the spans passes the K–S test. With the increase in the span, the maximum and average asymptotic significance level would decrease to 0. Since that the significance level with a span of 4 h is quite close to that with span of 6 h and there may be longer queue length due to less appointment periods with span of 6 h, we select 4 h as the appropriate span. The numbers of trucks during a day are given in Table 4 below.

Table 4. Number of trucks in each appointment period.

Number	Appointment Period					
	[0, 4]	**[4, 8]**	**[8, 12]**	**[12, 16]**	**[16, 20]**	**[20, 24]**
λ_1 (SL)	29.99	15.85	15.55	38.90	47.40	40.75
λ_2 (SE)	15.25	7.88	22.72	36.63	35.38	27.12
λ_3 (TL)	27.43	16.90	20.73	23.70	38.68	39.34
λ_4 (TE)	28.72	24.13	20.81	24.59	26.50	27.89

5.2. Carbon Emissions Measurement

5.2.1. Unit Carbon Emissions Cost Settings

Carbon emissions generated by one truck in each second proposed in [29] is:

$$e = sp + \left(wav + 0.5C_d A\rho v^3 + wgC_r\ cos\theta v + wgv\ sin\theta v\right)/\varepsilon\eta \tag{24}$$

where s is the brake-specific fuel consumption, p is the engine power output, v is speed, w is weight, ρ is air density, θ is angle of slope, A is frontal surface area of the vehicle, g is gravity, C_r and C_d are the coefficients of rolling resistance and drag respectively, ε is vehicle drivetrain efficiency, and η is efficiency of engine. Then, the carbon emissions cost of each truck is $EC = ce$, where c is the price of unit carbon. Due to the variation of speed, it is difficult to use equation (21) to accurately calculate the carbon emissions of each truck. Thus, we intend to calculate the average carbon emissions of each type of trucks.

Based on the data of the seaport, we calculated the average weight of each type of truck as w, and, respectively, set the lowest speed (i.e., 0 km/h) and highest speed (usually, 20 km/h) as s. Based on Equation (21), and the value of the above parameters (see Appendix B) in [29], we calculated the carbon emissions $e\ (s = 0)$ and $e(s = 20)$, and took the average as the average carbon emissions of each type of trucks in each hour. Combing with the price of carbon in [30] (i.e., USD 24 per kg), the average carbon emissions cost of each type of trucks can be obtained. The results are summarized in Table 5.

Table 5. Unit carbon emissions cost.

Type of Trucks	Average Carbon Emissions Cost (USD/Hour)
SL	1.348
SE	1.034
TL	0.720
TE	0.720

SE—sending empty container, SL—sending loaded container, TE—taking empty container and TL— taking loaded container.

We added up the products of average carbon emissions cost times number of each type of trucks, and then divided the total number of four types of trucks to obtain the average carbon emission cost (i.e., c_o), which is USD 0.954 per hour.

5.2.2. Evaluating Carbon Emissions Policy on Seaport Decision

This section focused on the effect of government policy on lane allocation decisions and total cost. We vary the unit carbon emissions cost by increasing R times as the average carbon emission cost (i.e., c_o). The bigger the R is, the stricter the government policy is. Specifically, R is set as 1 (i.e., the baseline case), 5, 10, 25, 50 and 100, respectively. The optimal allocated lanes for each type of truck in each appointment period are shown in Table 6.

Table 6. Solution of the lane allocation under different emission policy.

	Appointment Period	SE	SL	TE	TL
R = 1	[0, 4]	1	2	2	2
	[4, 8]	1	1	1	1
	[8, 12]	1	1	1	2
	[12, 16]	2	2	1	2
	[16, 20]	2	2	1	2
	[20, 24]	2	2	2	2
	Appointment Period	**SE**	**SL**	**TE**	**TL**
R = 5	[0, 4]	1	2	2	2
	[4, 8]	1	1	1	1
	[8, 12]	1	1	1	2
	[12, 16]	2	2	1	2
	[16, 20]	2	2	1	2
	[20, 24]	2	2	2	2
	Appointment Period	**SE**	**SL**	**TE**	**TL**
R = 10	[0, 4]	1	2	2	2
	[4, 8]	1	1	1	1
	[8, 12]	1	1	1	2
	[12, 16]	2	2	1	2
	[16, 20]	2	2	2	2
	[20, 24]	2	2	2	2
	Appointment Period	**SE**	**SL**	**TE**	**TL**
R = 25	[0, 4]	1	2	2	2
	[4, 8]	1	1	1	1
	[8, 12]	1	1	1	2
	[12, 16]	2	2	1	2
	[16, 20]	2	2	2	2
	[20, 24]	2	2	2	2
	Appointment Period	**SE**	**SL**	**TE**	**TL**
R = 50	[0, 4]	1	2	2	2
	[4, 8]	1	1	1	1
	[8, 12]	1	2	1	2
	[12, 16]	2	2	2	2
	[16, 20]	2	2	2	2
	[20, 24]	2	2	2	2
	Appointment Period	**SE**	**SL**	**TE**	**TL**
R = 100	[0, 4]	1	2	2	2
	[4, 8]	1	1	2	2
	[8, 12]	1	2	1	2
	[12, 16]	2	2	2	2
	[16, 20]	2	2	2	2
	[20, 24]	2	2	2	2

R—coefficient of average carbon emission cost, SE—sending empty container, SL—sending loaded container, TE—taking empty container and TL— taking loaded container.

As R increases, there are more lanes opened, especially for trucks of type SL and TL. Compared with the trucks of type SE and TE, the trucks of type SL and TL are heavier in weight, thus generating more carbon emissions while idling or moving. In order to reduce carbon emissions and therefore carbon emissions cost, more lanes would be opened to relieve congestion in the gate.

With the increase in R, the total cost would increase, which is shown in Table 7 and Figure 4.

Table 7. Total cost under different emission policy.

R	1	5	10	25	50	100
Total Cost (USD)	3047.3	3912.9	4411.8	6023.5	10127.4	27192.0

R—coefficient of average carbon emission cost.

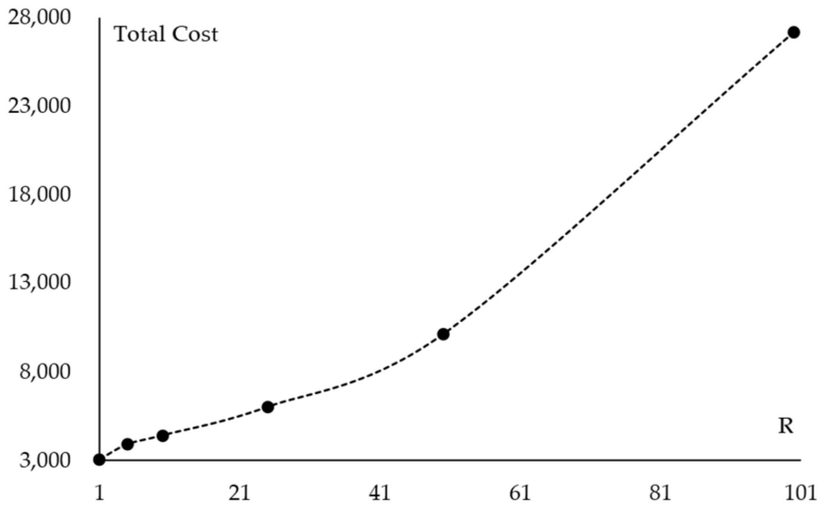

Figure 4. Effect of emission policy on total cost.

5.3. Sensitivity Analysis about Scale of Lanes

This section focuses on the effect of the scale of lanes on seaport operations. We varied the scale for 8 to 12. The findings are summarized in Table 8. As the scale increases, the total cost decreases. Obviously, increasing the scale of lanes would lead to a less total cost. The most probable cause is that the decrease in marginal carbon emissions cost is faster than the increase in marginal operation cost due to the growth of scale. As shown in Figure 5, the total cost is minimal when the scale is 11, and the total cost remains unchanged when the scale continues to increase. Thus, the optimal scale of lanes is 11. Due to the current scale being 8, the seaport could appropriately invest the gate to increase the scale of lanes to 11 to achieve optimal operation.

Table 8. Total cost under different scale of lanes.

Scale of Lanes	8	9	10	11	12
Total Cost (USD)	3047.3	2984.5	2966.5	2909.5	2909.5

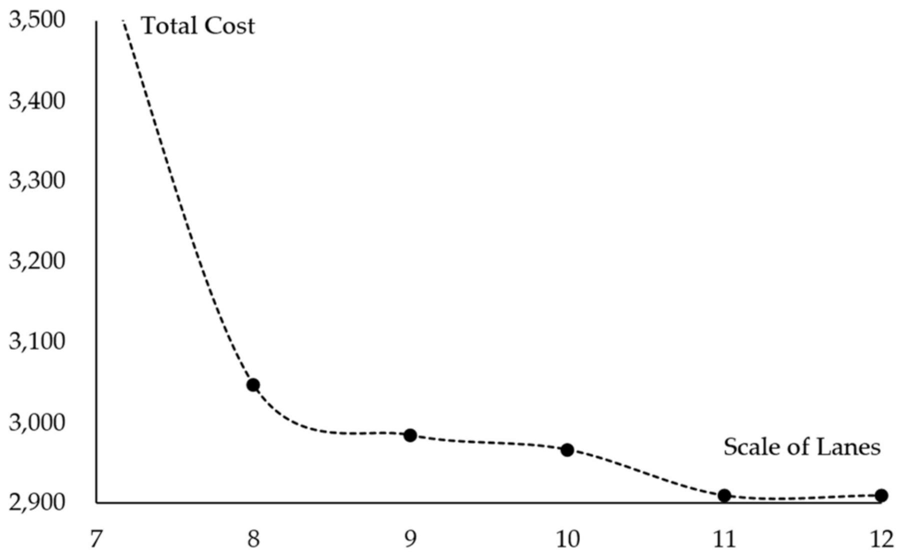

Figure 5. Effect of scale of lanes on total cost.

5.4. Computational Performance Analysis

This paper used MATLAB R2018a to implement the proposed algorithm and model, and all experiments in this paper were evaluated on PCs with Intel(R) Core (TM) i7-4710MQ CPU @2.50 GHz and a memory of 8.0 GB. Table 9 shows the computational time for cases in Sections 5.2.2 and 5.3. All the computational times are less than 120 s. Based on the requirements of solving the time limitation (less in 7.5 min) proposed in [39], the proposed algorithm is effective to deal with lane allocation problems in seaports.

Table 9. Computational time.

Section 5.2.2	R	1	5	10	25	50	100
	Time (s)	102	89	86	86	91	88
Section 5.3	Lane Scale	8	9	10	11	12	
	Time (s)	88	109	156	169	202	

6. Conclusions

At container seaports, the service demand of arrival trucks and the service supply of lanes are not always balanced, resulting in long queues of trucks and carbon emissions at the gate. In order to alleviate gate congestion, this paper focuses on lane allocation decisions combining with TAS, in order to minimize the total cost including the operation cost and carbon emissions cost. The resulting model is a nonlinear fractional integer programming. We first equivalently transformed it into an integer programming with bilinear constraints, and then proposed an improved branch-and-bound algorithm to solve it.

The numerical study and comparative analysis confirmed the validity of the proposed model and algorithm. In order to relieve congestion and reduce carbon emissions, more lanes could be allocated, especially for trucks of the type to send a loaded container and take a loaded container. The seaport could increase investment properly to build more lanes and further improve operations.

In this work, the lane allocation problem focused on arrival trucks and does not involve the departure trucks. Future studies will consider the joint allocation problem of arrival and departure trucks. In addition, the weather condition could be considered in the lane allocation problem.

Author Contributions: Conceptualization, Z.J. and X.L.; methodology, X.L.; software, W.L.; validation, L.Z.; formal analysis, X.L.; investigation, L.Z.; resources, L.Z.; data curation, X.L.; writing—original draft preparation, X.L.; writing—review and editing, W.L.; visualization, L.Z.; supervision, W.L.; project administration, Z.J. and X.X.; funding acquisition, Z.J. and X.X. All authors have read and agreed to the published version of the manuscript.

Funding: This research is partially supported by the Belt & Road Program of China Association for Science and Technology (2020ZZGJB072032), Joint Program of Liaoning Provincial Natural Science Foundation of China (2020HYLH49), Leading Talents Support Program of Dalian Municipal Government (2018-573), Fundamental Research Funds for the Central Universities (3132019301), National Natural Science Foundation of China (71572023) and European Commission Horizon 2020 (MSCA-RISE-777742-56). This research is partially supported by the National Key R&D Program of China (2019YFB1404901), the National Natural Science Foundation of China (71821002) and the National Training Program of Innovation and Entrepreneurship for Undergraduates of China (202010335011). This research is also partially supported by Guizhou Science Contract (201920013).

Institutional Review Board Statement: Not applicable.

Informed Consent Statement: Not applicable.

Data Availability Statement: Data sharing is not applicable to this article.

Acknowledgments: The authors would like to thank the strong administration support rendered by the MDPI editorial team.

Conflicts of Interest: The authors declare no conflict of interest.

Appendix A

Table A1. K–S test for the distribution of service time.

Type of Trucks		SL	SE	TL	TE
Record Number		24106	18581	21357	19538
Average Service Time [1]		37.85	39.09	49.36	34.39
Exp. Para. [2]		2.52	2.61	3.29	2.29
Distance	Abs.	0.124	0.234	0.231	0.256
	Positive	0.042	0.065	0.060	0.085
	Negative	−0.124	−0.234	−0.231	−0.256
K–S Test Result		16.86	36.34	32.25	37.45
Asymptotic Significance		0.012	0.006	0.030	0.004

[1] The average service time is reported in minutes. [2] Exp. Para. is reported in minutes.

Table A2. K–S test for the distribution of arrival time under different span.

Type	Item	1 h	2 h	3 h	4 h	6 h
SL	Max. [1]	0.750	0.063	0.001	<0.001	<0.001
	Avg. [2]	0.049	0.015	0.001	<0.001	<0.001
	Over Num. [3]	3	1	0	0	0
	>0.05 (%) [4]	12.50	8.33	0.00	0.00	0.00
SE	Max.	0.541	0.263	0.088	0.002	<0.001
	Avg.	0.099	0.025	0.012	0.001	<0.001
	Over Num.	8	1	1	0	0
	>0.05 (%)	33.33	8.33	12.50	0.00	0.00
TL	Max.	0.519	0.766	0.469	0.004	<0.001
	Avg.	0.118	0.079	0.059	0.001	<0.001
	Over Num.	9	3	1	0	0
	>0.05 (%)	37.50	12.50	12.50	0.00	0.00

Table A2. *Cont.*

Type	Item	1 h	2 h	3 h	4 h	6 h
TE	Max.	0.056	<0.001	<0.001	<0.001	<0.001
	Avg.	0.003	<0.001	<0.001	<0.001	<0.001
	Over Num.	1	0	0	0	0
	>0.05 (%)	4.17	0.00	0.00	0.00	0.00

[1] The max confidence level among all the appointment periods. [2] The average confidence level among all the appointment periods. [3] The numbers of group whose K–S test confidence level are less than 95%. [4] The percentage of group whose K–S test asymptotic significance level are more than 0.05.

Appendix B

$s = 70\ (\text{kw})$, $p = 220\ (\text{g/KW.hr})$, $\theta = 0$, $v = 5(\text{m/s})$, $a = 0\ \left(\text{m}^2/\text{s}\right)$, $A = 4\ \left(\text{m}^3\right)$, $g = 9.788\ \left(\text{m}^2/\text{s}\right)$, $C_r = 0.012$, $C_d = 0.9$, $\rho = 1.293\ \left(\text{kg/m}^3\right)$, $\varepsilon = 0.9$, $\eta = 0.45$.

References

1. Shi, X.; Vanelslander, T. Design and evaluation of transportation networks: Constructing transportation networks from perspectives of service integration. *NETNOMICS Econ. Res. Electron. Netw.* **2010**, *11*, 1–4. [CrossRef]
2. Shi, X.; Stefan, V. Container terminal operations under the influence of shipping alliances. In *Risk Management in Port Operations, Logistics and Supply Chain Security*, 1st ed.; Khalid, B., Michael, G., Eds.; Informa: London, UK, 2007; pp. 135–167.
3. Smith, T.; Jalkanen, J.; Anderson, B.; Corbett, J.; Faber, J.; Hanayama, S.; O'Keeffe, E.; Parker, S.; Johansson, L.; Aldous, L.; et al. *Third IMO GHG Study*; International Maritime Organization: London, UK, 2014.
4. Wang, S.; Zhen, L.; Harilaos, N. Three potential benefits of the EU and IMO's landmark efforts to monitor carbon dioxide emissions from shipping. *Front. Eng. Manag.* **2020**, *1*, 1–2. [CrossRef]
5. Zhuge, D.; Wang, S.; Zhen, L.; Laporte, G. Subsidy design in a vessel speed reduction incentive program under government policies. *Nav. Res. Logist.* **2020**, *68*, 344–358. [CrossRef]
6. Zhen, L.; Li, M.; Hu, Z.; Lv, W.; Zhao, X. The effects of emission control area regulations on cruise shipping. *Transp. Res. Part D Transp. Environ.* **2018**, *62*, 47–63. [CrossRef]
7. Zhen, L.; Hu, Z.; Yan, R.; Zhuge, D.; Wang, S. Route and speed optimization for liner ships under emission control policies. *Transp. Res. Part C Emer. Technol.* **2020**, *110*, 330–345. [CrossRef]
8. Zhen, L.; Wu, Y.; Wang, S.; Laporte, G. Green technology adoption for fleet deployment in a shipping network. *Transp. Res. Part B Methodol.* **2020**, *139*, 388–410. [CrossRef]
9. Du, Y.; Chen, Q.; Quan, X.; Long, L.; Fung, R. Berth allocation considering fuel consumption and vessel emissions. *Transp. Res. Part E Logist. Transp. Rev.* **2011**, *47*, 1021–1037. [CrossRef]
10. Zhen, L.; Sun, Q.; Zhang, W.; Wang, K.; Yi, W. Column generation for low carbon berth allocation under uncertainty. *J. Oper. Res. Soc.* **2020**, 1–16. [CrossRef]
11. Venturini, G.; Iris, C.; Kontovas, C.; Larsen, A. Multi-port berth allocation problem with speed optimization and emission considerations. *Transp. Res. Part D Transp. Environ.* **2017**, *54*, 142–159. [CrossRef]
12. Sun, Q.; Zhen, L.; Xiao, L.; Tan, Z. Recoverable robustness considering carbon tax in weekly berth and quay crane planning. In *Smart Transportation Systems 2019, Smart Innovation, Systems and Technologies*, 1st ed.; Qu, X., Zhen, L., Eds.; Springer: Singapore, 2019; Volume 149, pp. 75–84.
13. Talavera, A.; Barron, J.; Passamani, C. Optimization of vessel and quay crane emissions during the hoteling phase. In Proceedings of the 7th International Conference on Information, Intelligence, Systems & Applications, Chalkidiki, Greece, 13–15 July 2016; IEEE: Piscataway Township, NJ, USA, 2016; pp. 1–10.
14. Sha, M.; Zhang, T.; Lan, Y.; Zhou, X.; Qin, T.; Yu, D.; Chen, K. Scheduling optimization of yard cranes with minimal energy consumption at container terminals. *Comput. Ind. Eng.* **2017**, *113*, 704–713. [CrossRef]
15. Peng, Y.; Wang, W.; Song, X.; Zhang, Q. Optimal allocation of resources for yard crane network management to minimize carbon dioxide emissions. *J. Clean. Prod.* **2016**, *131*, 649–658. [CrossRef]
16. Kavakeb, S.; Nguyen, T.; McGinley, K.; Yang, Z.; Jenkinson, I.; Murray, R. Green vehicle technology to enhance the performance of a European port: A simulation model with a cost-benefit approach. *Transp. Res. Part C Emer. Technol.* **2015**, *60*, 169–188. [CrossRef]
17. Yu, H.; Ge, Y.; Chen, J.; Luo, L.; Tan, C.; Liu, D. CO_2 emission evaluation of yard tractors during loading at container terminals. *Transp. Res. Part D Transp. Environ.* **2017**, *53*, 17–36. [CrossRef]
18. Facchini, F.; Boenzi, F.; Digiesi, S.; Mummolo, G. A model-based decision support system for multiple container terminals hub management. *Production* **2018**, *28*, 1–12. [CrossRef]
19. Digiesi, S.; Facchini, F.; Mummolo, G. Dry Port as a lean and green strategy in a container terminal hub: A mathematical programming model. *Manag. Prod. Eng. Rev.* **2018**, *10*, 14–28.
20. Kurtulus, E.; Cetin, I.B. Assessing the environmental benefits of dry port usage: A case of inland container transport in Turkey. *Sustainability* **2019**, *11*, 6793. [CrossRef]

21. Yang, H.; Lin, X.; Xu, L.; Li, X.; Jin, Z.; Bian, Z. Truck appointment at container terminals: Status and perspectives. In Proceedings of the 30th Chinese Control and Decision Conference, Shenyang, China, 9–11 June 2018; IEEE: Piscataway Township, NJ, USA, 2018; pp. 1954–1960.
22. Yang, H.; Shao, Q.; Gen, F.; Jin, Z. Collaborative optimization of yard crane deployment and truck appointment based on two-way transmission of information. *J. Dalian. Marit. Univ.* **2017**, *43*, 29–38.
23. Hu, L.; Shi, X.; Voß, S.; Zhang, W. Application of RFID technology at the entrance gate of container terminals. *Comput. Logist.* **2011**, *6971*, 209–220.
24. Shi, X.; Tao, D.; Voß, S. RFID technology and its application to port-based container logistics. *J. Organ. Comput. Electron. Commer.* **2011**, *21*, 332–347. [CrossRef]
25. Zhen, L. Tactical berth allocation under uncertainty. *Euro. J. Oper. Res.* **2015**, *247*, 928–944. [CrossRef]
26. Li, N.; Chen, G.; Ng, M.; Talley, K.; Jin, Z. Optimized appointment scheduling for export container deliveries at marine terminals. *Marit. Policy Manag.* **2019**, *47*, 1–23. [CrossRef]
27. Fan, H.; Ren, X.; Guo, Z.; Li, Y. Truck scheduling problem considering carbon emissions under truck appointment system. *Sustainability* **2019**, *11*, 6256. [CrossRef]
28. Yu, M.; Zhou, M. Optimization model of delivery container truck appointment based on gate resource allocation. *J. Wuhan. Univ. Technol. (Transp. Sci. Eng.)* **2020**, *44*, 648–652.
29. Bektas, T.; Laporte, G. The pollution-routing problem. *Transp. Res. Part B Methodol.* **2011**, *45*, 1232–1250. [CrossRef]
30. Ricke, K.; Drouet, L.; Caldeira, K.; Tavoni, M. Country-level social cost of carbon. *Nat. Clim. Chang.* **2018**, *8*, 895–900. [CrossRef]
31. Zeng, Q.; Chen, W.; Hu, X. Optimization model and algorithms of truck appointment in container terminals. *Chin. J. Manag. Sci.* **2015**, *23*, 125–130.
32. Ma, M.; Fan, H.; Jiang, X.; Guo, Z. Truck arrivals scheduling with vessel dependent time windows to reduce carbon emissions. *Sustainability* **2019**, *11*, 6410. [CrossRef]
33. Phan, M.; Kim, K. Collaborative truck scheduling and appointments for trucking companies and container terminals. *Transp. Res. Part B Methodol.* **2016**, *86*, 37–50. [CrossRef]
34. Im, H.; Yu, J.; Lee, C. Truck appointment system for cooperation between the transport companies and the terminal operator at container terminals. *Appl. Sci.* **2021**, *11*, 168. [CrossRef]
35. Li, N.; Chen, G.; Govindan, K.; Jin, Z. Disruption management for truck appointment system at a container terminal: A green initiative. *Transp. Res. Part D Transp. Environ.* **2015**, *61*, 261–273. [CrossRef]
36. Shao, Q.; Jin, Z.; Xing, L. Simulation optimization of consolidation and configuration in container terminals based on cooperative appointment. *J. Transp. Syst. Eng. Inf. Technol.* **2016**, *16*, 217–224.
37. Torkjazi, M.; Huynh, N.; Shiri, S. Truck appointment systems considering impact to drayage truck tours. *Transp. Res. Part E Logist. Transp. Rev.* **2018**, *116*, 1021–1037. [CrossRef]
38. McCormick, G. Computability of global solutions to factorable nonconvex programs: Part I-convex underestimating problems. *Math. Program.* **1976**, *10*, 147–175. [CrossRef]
39. Wasesa, M.; Stam, A.; Heck, E. The seaport service rate prediction system: Using drayage truck trajectory data to predict seaport service rates. *Decis. Support Syst.* **2017**, *95*, 37–48. [CrossRef]